Available online at www.sciencedirect.com
SCIENCE DIRECT
Journal of Catalysis 228 (2004) 243–253
JOURNAL OF CATALYSIS
www.elsevier.com/locate/jcat

Influence of reductant on the regeneration of SO_2-poisoned $Pt/Ba/Al_2O_3$ NO_x storage and reduction catalyst

Zhaoqiong Liu, James A. Anderson *

Surface Chemistry and Catalysis Group, Division of Physical and Inorganic Chemistry, University of Dundee, DD1 4HN, Scotland, UK

Received 9 June 2004; revised 27 August 2004; accepted 3 September 2004

Abstract

A 10% Ba/Al_2O_3 in the presence and absence of 1% Pt was exposed to SO_2 at 673 K either in air or in nitrogen, and the ability to recover the NO_x storage capacity was compared after exposure to H_2, CO, or C_3H_6 at 673 K. Exposure to SO_2 led to adsorbed sulfite, surface aluminum sulfate, and bulk and surface barium sulfate formation, all of which reduced the NO_x storage capacity of the catalyst. The presence of Pt was required for bulk barium sulfate formation. A surface aluminum sulfate was formed from surface sulfite species to a limiting extent at 673 K but this was enhanced by heating in air to higher temperatures and was thermally stable up to 873 K. In the case of the Pt-containing catalyst, hydrogen at 673 K was able to completely reverse the detrimental effect of SO_2 exposure whereas H_2 exposure to SO_2-treated Pt-free catalyst was detrimental in terms of recovered NO_x storage capacity. The presence of oxygen in the feed stream during the rich regeneration period was significant as this allowed formation of water (and CO_2) which plays an important role in the regeneration process.

Keywords: NSR catalysts; NO_x trap; $Pt/Ba/Al_2O_3$; SO_2 poisoning; Catalyst regeneration

1. Introduction

Storage and reduction catalysts (NSR) allow control of NO_x emissions from automobile sources while permitting operation under predominantly lean-burn conditions [1–8]. The concept is based on the storage of NO_x under lean conditions on an alkaline earth oxide component such as baria which is then released during intermittent rich/stoichiometric periods where the stored NO_x is released and reduced by H_2, CO, or HC over the noble metal component. The NO_x storage capacity of NSR catalysts are lowered as a function of time on stream as sulfate is accumulated on the storage component [3–8]. In cases where the extent of deactivation is relatively low, NO_x storage capacity may be readily regenerated under reducing conditions [9]. In more severe cases, even extended regeneration periods fail to recover the initial storage capacity [3,9]. This transition in the ease by which sulfate may be removed may be associated with the transition from surface to bulk sulfates [4], although this is difficult to envisage as bulk barium carbonate still retains NO_x storage ability and it is generally accepted that NO_x storage is a surface rather than a bulk phenomenon [10,11]. It is also possible that sulfate particle size governs the ease by which this phase is decomposed [12]. It is generally considered that temperatures of between 723 and 823 K are required [5] and so failure to recover catalyst performance following desulfation may result from thermal degradation of the catalyst [5,6]. The difficulty in achieving complete regeneration following sulfate poisoning may also be linked to the regeneration procedure employed as these invariably involve exposure of the catalyst to a reducing atmosphere at high temperature [5] which may induce sulfide formation [3]. Although some of this sulfide is associated with Ba [3] there is also evidence that sulfide becomes associated with the metallic component [4,13] which therefore hinders further regeneration via reduction.

During the fuel-rich step, lean-burn engines emit CO (5–6%), H_2 (1–2%), and hydrocarbons (ppm levels), al-

* Corresponding author.
E-mail address: j.a.anderson@dundee.ac.uk (J.A. Anderson).

0021-9517/$ – see front matter
doi:10.1016/j.jcat.2004.09.004

though the relative concentrations can be modified by engine management or insertion of a precatalyst. For example, hydrogen levels might be increased by water–gas shift or steam-reforming reactions. To shed further light on the deactivation and regeneration processes, the current study involved the use of CO, H_2, and C_3H_6 as reductants to examine the efficiency of trap regeneration for Ba/Al_2O_3 traps in the presence and absence of Pt which had been exposed to SO_2 either in air or in nitrogen. The objective was to determine whether sulphate buildup could be minimised, thereby limiting barium sulfate particle-size growth by selection of the appropriate conditions during the NO_x reduction cycles which would remove stored SO_x at each rich switch and thereby avoid progressive SO_x accumulation, loss of NO_x storage capacity, and the need to use high-temperature-rich excursions [5] to eliminate stable sulfates. The choice of NO_2 rather than NO allowed an investigation of SO_2 poisoning of support sites to be conducted by avoiding the need for Pt-catalysed oxidation as the latter might potentially become poisoned by SO_2 [4,13], leading to ambiguity regarding the origin of reduced NO_x uptakes.

2. Experimental

BaO/Al_2O_3 samples (10 wt% BaO) were prepared by precipitation of $Ba(OH)_2$ from a nitrate solution onto Degussa Aluminiumoxid C using an ammonia solution. The material was filtered, washed, dried at 363 K (16 h), and calcined in air at 773 K (2 h). A portion of the sample was wet impregnated with 1 wt% Pt (H_2PtCl_6) and excess water removed by heating while continually stirring. The resulting powder was dried overnight at 363 K and calcined in air (100 $cm^3\,min^{-1}$) at 773 K (2 h). To distinguish between the influence of Pt and the influence of baria dispersion which is modified as a consequence of the addition of Pt precursor [14–16], a portion of the Ba/Al_2O_3 support was treated with HCl solution (pH 1.2) and then dried overnight at 363 K and washed with ammonia solution (pH 8.5). This sample is referred to as "HCl-treated support." It is clear [14] that the presence of this Cl may influence the adsorption properties of the support.

Samples for XRD purposes were calcined at 673 K and then exposed to 0.28 mmol of SO_2 at the same temperature followed by cooling in air to 298 K. One of the samples for XRD was regenerated with 3.35% H_2/4% air/balance N_2 mixture after SO_2 exposure at 673 K for 5 min and then cooling in air to 298 K. XRD patterns were obtained using a Philips PW1310 X-ray generator, using Cu-Kα radiation ($\lambda = 1.542$ Å), coupled to a Philips PW1964 scintillation counter.

DRIFT spectra (4 cm^{-1} resolution, 40 scans, MCT detector) were recorded using ca. 80-mg sample in a Harrick environmental cell. A gas blender fed the inlet gases, with exit gas analysis performed using on-line chemiluminescence (NO/NO_2) and Quadrupole mass spectrometer. Samples were calcined in situ (673 K, 1 h, 50 $cm^3\,min^{-1}$). SO_2 was injected as a series of 7×1 cm^3 pulses either in flowing air or in N_2, and then the catalyst was either directly exposed to NO_2 or first exposed to a regeneration procedure which involved treatment in a flow containing H_2, CO, or propene under rich conditions. Gas mixtures contained 3.35% H_2 (or CO)/4% air/balance N_2 or 7.10% of 5% propene in N_2/4% air/balance N_2. Samples were exposed to NO_2 (750 ppm) at 673 K for 15 min and then cooled to 298 K in NO_2 before flushing in air for ca. 15 min to remove gaseous and weakly adsorbed forms of NO_x as indicated by the detector returning to background levels. A TPRS was performed between 298 and 873 K at 4 K min^{-1} in 7.98% air/N_2 (50 $cm^3\,min^{-1}$) to determine the amount of stored NO_x.

3. Results

3.1. Sample characteristics

Ba/Al_2O_3 exhibited (2θ) peaks at 24.1, 34.7, and 42.1° due to $BaCO_3$ and at 19.4, 22.0, and 28.0° due to $BaAl_2O_4$ [14,17] (Fig. 1a). There was no obvious change after exposure to SO_2 (Fig. 1b) (peaks at $2\theta = 44.6$ and 38.3 are due to Al holder). $Pt/Ba/Al_2O_3$ displayed only features due to alumina, although the presence of minor, weaker diffraction lines due to $BaCO_3$ and $BaAl_2O_4$ cannot be ruled out. Following SO_2 treatment, additional peaks at 26.0, 28.7, and 42.5° appeared due to the presence of $BaSO_4$ [18]. These features were almost completely removed by H_2 treatment at 673 K (Fig. 1e).

3.2. Combined TPRS/FTIR experiments: Pt-containing catalysts

NO_2 was the dominant gas released by SO_x-free $Pt/Ba/Al_2O_3$ (Fig. 2a) giving maxima at 350, 530, and 729 K.

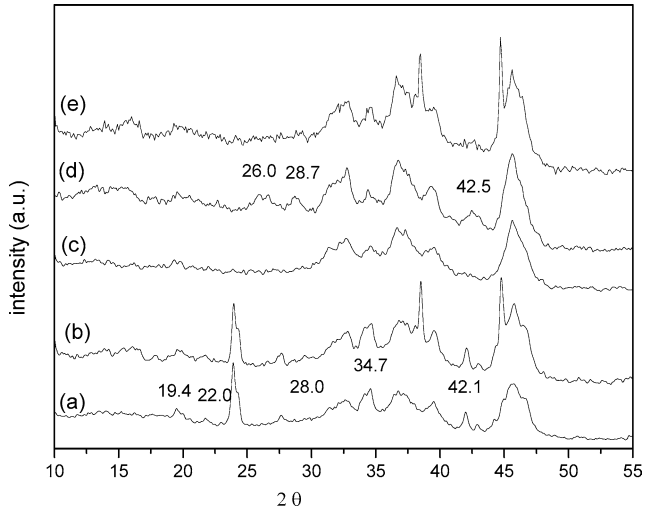

Fig. 1. XRD patterns of samples before and after SO_2 treatment at 673 K. Ba/Al_2O_3 (a) before and (b) after SO_2 treatment and $Pt/Ba/Al_2O_3$ (c) before, (d) after SO_2 treatment, and (e) after H_2 regeneration.

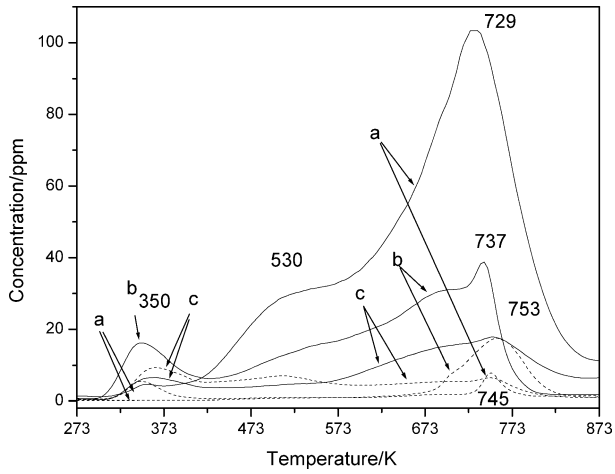

Fig. 2. TPRS of NO (dashed line) and NO_2 (solid line) released from $Pt/Ba/Al_2O_3$ on sample (a) without SO_2 treatment, (b) after SO_2 treatment in N_2, and (c) after SO_2 treatment in air and then exposure to 750 ppm NO_2 in N_2/air at 673 K and cooled to 298 K, and then heated to 873 K at 4 K min^{-1} in a 7.98% air/balance N_2 gas mixture (50 cm^3 min^{-1}).

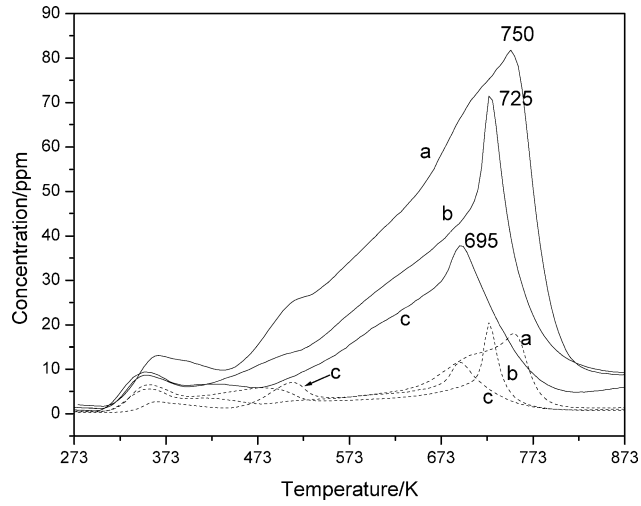

Fig. 3. TPRS of NO (dashed line) and NO_2 (solid line) released from $Pt/Ba/Al_2O_3$ after exposure to 750 ppm NO_2 in N_2/air at 673 K and cooled to 298 K, and then heated to 873 K at 4 K min^{-1} in a 7.98% air/balance N_2 gas mixture (50 cm^3 min^{-1}) on samples which had been exposed to SO_2 in air at 673 K and then regenerated with (a) H_2, (b) CO, or (c) C_3H_6.

NO was released in a single peak at 745 K. For catalysts which had been exposed to SO_2 either in N_2 or in air, the TPRS profiles (Fig. 2b and 2c) were similar to the SO_2-free sample, except that intensities of peaks were diminished for catalysts which had been exposed to SO_2. The exception was the maxima at 350 K which was increased for samples exposed to SO_2 in either air or N_2. Another characteristic of the NO_2 desorption profile was that the peak of maximum intensity was shifted from 729 to 737 K for sample treated in SO_2/N_2 and to 753 K for sample treated in SO_2/air. In the case of the NO profiles, the most significant difference between SO_2-free and SO_2-treated samples were the appearance of a maximum at ca. 350 K for the latter.

Although varying degrees of efficiency were achieved in terms of catalyst regeneration, the shapes of desorption profiles were similarly independent of the reductant used (Fig. 3). NO_2 was the predominant NO_x gas irrespective of the reductant employed. NO was released as the minor component in all cases, at a temperature which corresponded with the maximum in the NO_2 profile. Sample exposed to H_2 (Fig. 3a) gave the most intense NO_2 peak, indicating that regeneration of the NO_x storage capacity had been most successful using this gas. Sample exposed to C_3H_6 gave the least intense NO_2 peak (Fig. 3c), indicating that it was the least effective reductant for NO_x storage capacity regeneration. The NO released was much less than NO_2, but also followed the trend that the amount released was greatest following H_2 treatment and lowest after C_3H_6 treatment (Table 1). The peak maxima of the NO_2 profile was shifted from 750 to 725 K for the sample treated with H_2 and CO and to 695 K for the sample treated with C_3H_6.

NO_x released (% of total NO_x capacity) from different pretreated $Pt/Ba/Al_2O_3$ is summarised in Fig. 4. Storage capacity was significantly decreased after exposure to SO_2 in

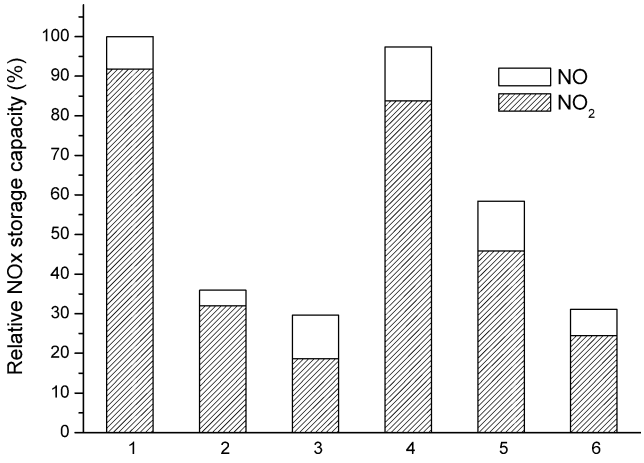

Fig. 4. Summary of the relative amounts of NO_x released from different pretreated $Pt/Ba/Al_2O_3$ samples as a percentage of total NO_x released from fresh sample. (1) Fresh sample, (2) exposed to SO_2/N_2, exposed to SO_2/air with (3) no regeneration, or (4) regenerated with H_2 or (5) regenerated with CO or (6) regenerated with C_3H_6.

air (30%) or in N_2 (36%). The storage capacity could be almost completely recovered (97.4%) using H_2 as reductant at 673 K. When this sample underwent repeated cycles of SO_2 exposure/hydrogen regeneration/NO_2 adsorption (up to 5 cycles), the total NO_x uptake never fell below 95% (with respect to the fresh catalyst). The other reductant gases were less efficient with CO regeneration recovering 58.4% of the original capacity. C_3H_6 regeneration proved to be least effective (31.2%), with recovery being only marginally higher than for catalysts which had not undergone regeneration (30%).

DRIFTS spectra of samples after exposure to NO_2 at 673 K are shown in Fig. 5. Bands at 1432 and 1320 cm^{-1} are consistent with results for previous studies and were ob-

Table 1
Summary of NO_x released during TPRS experiments

Pretreatment	NO_2 (mmol/g_{cat}) (T_{max} (K))				NO (mmol/g_{cat})	NO_x[a] (mmol/g_{cat})
	Peak 1	Peaks 2, 3	Peaks 3, 4	Total[a]		
Without SO_2	0.0056 (326)	0.175 (573)	0.257 (735)	(0.438) 0.424	0.038 (760)	(0.475) 0.462
SO_2 in N_2	0.0182 (360)	0.081(605)	0.0438 (723)	(0.143) 0.148	0.018 0.0075 (355) 0.0104 (753)	(0.161) 0.166
SO_2 in air	0.0059 (366)	0.0178 (482)	0.0752 (732)	(0.099) 0.086	0.051 0.0079 (370) 0.026 (500) 0.016 (723)	(0.150) 0.137
With H_2 regeneration	0.019 (370)	0.156 (580) 0.177 (717)	0.028 (750)	(0.380) 0.387	0.063	(0.443) 0.450
With CO regeneration	0.0145 (352)	0.166 (666)	0.025 (727)	0.210	0.058	0.268
With C_3H_6 regeneration	0.0083 (357)	0.0815 (646)	0.0153 (700)	(0.105) 0.113	0.031	(0.136) 0.144
Ba/Al_2O_3						
Without SO_2	0.0306 (356)		0.0748 (760)	(0.1054) 0.107	(0.098) 0.093 0.016 (355) 0.082 (800)	(0.203) 0.200
SO_2 in N_2	0.0022 (328)	0.04 (584)	0.09 (775)	0.132	0.074 (793)	0.202
SO_2 in air	0.0075 (346)	0.0238 (437) 0.0165 (602)	0.0286 (793)	(0.076) 0.054	0.069	(0.145) 0.123
With H_2 regeneration	0.011 (342)	0.007 (448) 0.017 (604)	0.040 (800)	0.075	0.01	0.085
With CO regeneration	0.018 (352)	0.012 (441) 0.023 (578)	0.055 (795)	(0.108) 0.102	0.009	(0.117) 0.111
With C_3H_6 regeneration	0.0015 (337)	0.062 (541)	0.048 (778)	0.111	0.015	0.126
HCl-treated Ba/Al_2O_3						
Without SO_2	0.004 (339)	0.107 (671)	0.065 (746)	0.176	0.03 (786)	0.206
SO_2 in N_2				0.111	0.033	0.144
SO_2 in air	0.011 (351)	0.013 (397) 0.032 (652)	0.007 (740)	(0.063) 0.088	0.008 (761)	(0.071) 0.096
With H_2 regeneration	0.0046 (382)	0.0308 (615)	0.0184 (749)	(0.054) 0.084	0.007	(0.061) 0.091
With CO regeneration	0.0093 (350)	0.015 (390) 0.037 (665)	0.009 (737)	(0.070) 0.092	0.015	(0.085) 0.107

[a] NO_x released calculated as the sum of the integrals of individual peaks or ( ) integral over the whole temperature range.

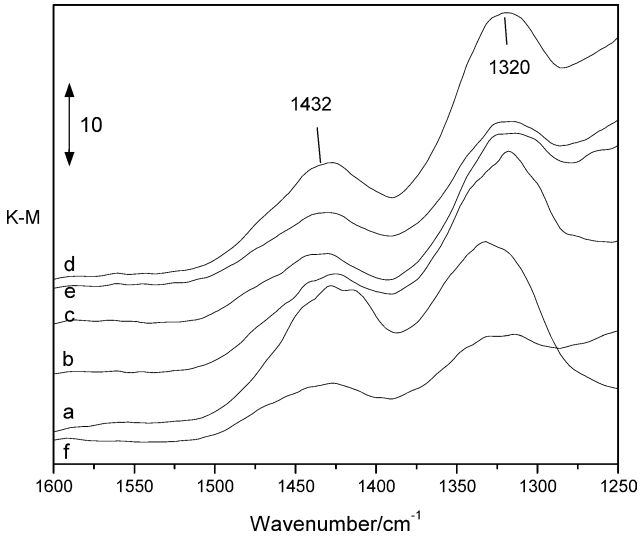

Fig. 5. FTIR spectra of $Pt/Ba/Al_2O_3$ after NO_2 adsorption at 673 and cooling to 298 K with different pretreated samples. (a) Without SO_2 treatment, (b) after SO_2 treatment at 673 K in N_2, or exposed to SO_2 in air at 673 K with subsequently (c) no regeneration, (d) regeneration in H_2, (e) regeneration in CO, and (f) regenerated in C_3H_6.

tained whether NO/O_2 mixtures or NO_2 were employed [6,14,17,19,20]. There were obvious differences in the intensities of this band pair after SO_2 exposure. After exposure to SO_2 in N_2, the intensity of the band at 1320 cm^{-1} appeared to increase and the component at 1432 cm^{-1} decreased compared with that of the SO_2-free sample. An increase in relative intensity at 1320 cm^{-1} was also found for sample exposed to SO_2 in air and again the intensity of the band at 1432 cm^{-1} was decreased. The intensity at 1432 cm^{-1} for the sample after H_2 treatment increased compared to sample without regeneration but without recovering the full intensity of the SO_2-free sample. However, after the same regeneration treatment, the intensity of the band at 1320 cm^{-1} was significantly increased compared to samples either with or without SO_2 exposure (Fig. 5d). Sample treated with CO showed similar trends but to a lesser extent than the effects observed for H_2. For sample regenerated with propene (Fig. 5f), both peaks appeared with slightly lesser intensity than for SO_2-treated (Fig. 5b and 5c) or SO_2-free (Fig. 5a) sample consistent with the lack of storage capacity regeneration using this reductant (Fig. 4).

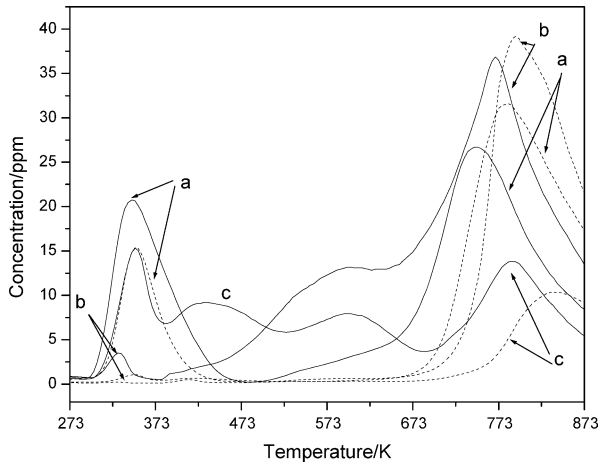

Fig. 6. TPRS of NO (dashed line) and NO_2 (solid line) released from support Ba/Al_2O_3 on sample (a) without SO_2 treatment, (b) after SO_2 treatment in N_2 at 673 K, or (c) after SO_2 treatment in air and then exposure to 750 ppm NO_2 in N_2/air at 673 K and cooled to 298 K and then heated to 873 K at 4 K min^{-1} in a 7.98% air/balance N_2 gas mixture (50 cm^3 min^{-1}).

3.3. Combined TPRS/FTIR experiments: Pt-free Ba/Al_2O_3 catalysts

Fig. 6 shows the NO_x TPRS profiles from Ba/Al_2O_3 which had either been directly exposed to NO_2 (Fig. 6a) or exposed to NO_2 after treatment in SO_2/N_2 (Fig. 6b) or SO_2/air (Fig. 6c). Ba/Al_2O_3 directly exposed to NO_2 (Fig. 6a) released NO_2 at 350, 600, and 745 K while NO was released at 350 and 782 K. For sample after exposure to SO_2 in N_2, the ratio of NO/NO_2 changed (Table 1) in favour of NO_2. This may have been a consequence of shifting peaks to higher temperature for both NO and NO_2 profiles with virtually no NO_x released at 350 K and a greater NO_2 release at ca. 600 K. Despite the differences in TPRS patterns, the stored NO_x was almost identical to the untreated sample (Table 1). Sample after exposure to SO_2 in air showed a decrease in the overall storage capacity (Table 1), although the peak at 350 K reappeared along with a new feature at 440 K (Fig. 6c). The peak at 600 K was of intermediate intensity between untreated and SO_2 in N_2-treated samples, but the high-temperature peak (788 K) was significantly reduced. NO was released only at the higher of the NO_2 desorption peaks.

NO_x desorption profiles from SO_2-pretreated sample after regeneration with H_2 or CO (Fig. 7a and 7b) were similar in shape to the profile of the TPRS profile with no regeneration (Fig. 6c), with NO_2 maxima at ca. 350, 440, 600, and 793 K. The main difference was the recovery of intensity at ca. 780 K using either H_2 or CO which would account for the partial recovery of the NO_x storage capacity (Table 1). Treatment in propene was less successful in recovering the intensity of the high-temperature feature (780 K) and the partial recovery of overall storage capacity (Table 1) was due to NO_x stored which was released in the mid-temperature range giving maxima at 450, 550, and 650 K (Fig. 7c). A feature observed at ca. 335 K, and also present for H_2 and

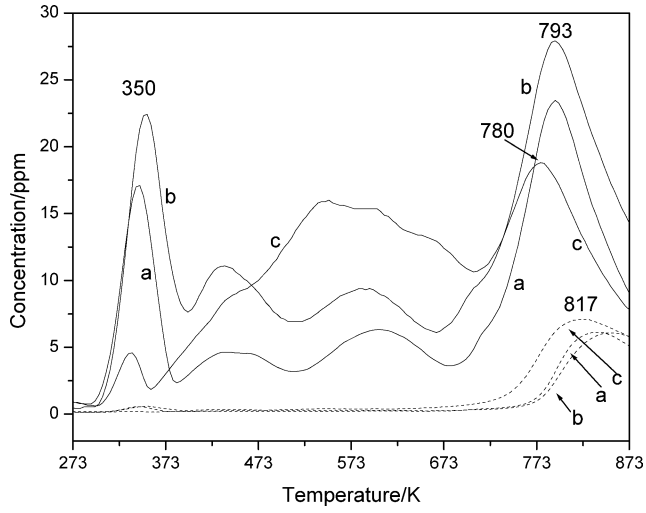

Fig. 7. TPRS of NO (dashed line) and NO_2 (solid line) released from support Ba/Al_2O_3 after exposure to 750 ppm NO_2 in N_2/air at 673 K and cooled to 298 K, and then heated to 873 K at 4 K min^{-1} in a 7.98% air/balance N_2 gas mixture (50 cm^3 min^{-1}) on samples which had been exposed to SO_2 in air at 673 K and then regenerated with (a) H_2, (b) CO, or (c) C_3H_6.

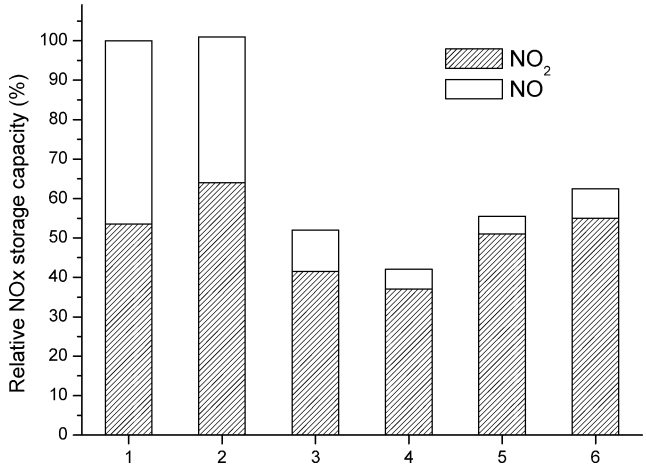

Fig. 8. Summary of the relative amounts of NO_x released from different pretreated supports as a percentage of total NO_x released from fresh sample. (1) Fresh sample, (2) exposed to SO_2/N_2 at 673 K or exposed to SO_2 in air at 673 K and either (3) no regeneration or (4) regenerated with H_2 or (5) regenerated with CO or (6) regenerated with C_3H_6.

CO-treated samples, was observed albeit of lesser intensity. A low intensity peak due to NO was observed at ca. 350 K. The majority of NO was released for all samples in a single peak around 830 K, irrespective of the reductant used to regenerate the catalyst.

NO_x released as a percentage of the original storage capacity for Ba/Al_2O_3 exposed to different treatments is summarised in Fig. 8. Unlike $Pt/Ba/Al_2O_3$ exposure of the support to SO_2/N_2 did not reduce the total NO_x storage capacity but did lead to a change in the NO/NO_2 ratio (53.5% NO_2 without SO_2 pretreatment, 64.0% NO_2 after exposure to SO_2 in N_2). Following exposure to SO_2 in air, the storage capacity of Ba/Al_2O_3 was decreased to 52% and subsequent

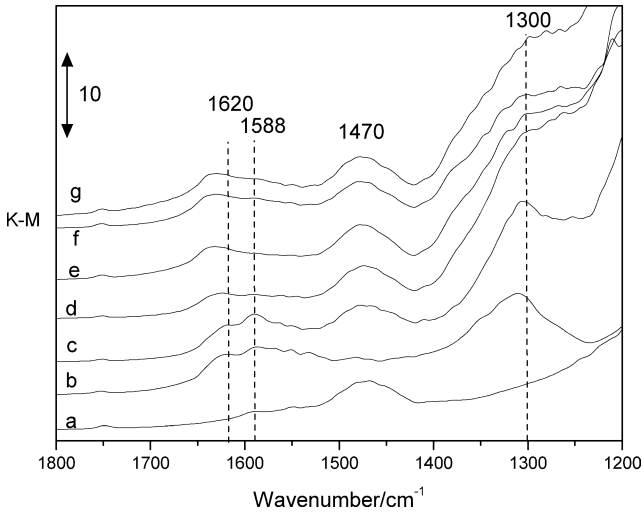

Fig. 9. FTIR spectra of support Ba/Al_2O_3 (a) before NO_2 adsorption, then after exposure to NO_2 at 673 K and cooling to 298 K with different pretreated sample (b) without SO_2, (c) after SO_2 treatment in N_2, or after exposure to SO_2 in air and (d) no regeneration, (e) regeneration in H_2, (f) regeneration in CO, (g) regeneration in C_3H_6.

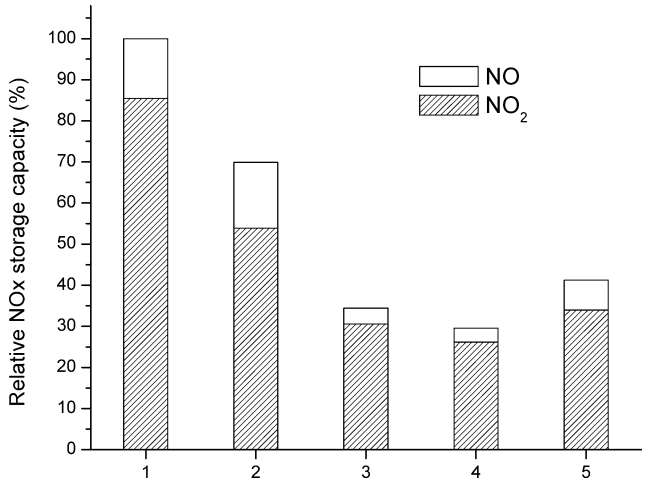

Fig. 10. Summary of the amounts of NO_x released from different pretreated supports as a percentage of total NO_x released from fresh treated support. (1) Fresh sample, (2) exposed to SO_2 in N_2 at 673 K or exposure to SO_2 in air with subsequently (3) no regeneration, or (4) regeneration with H_2 or (5) regeneration with CO.

H_2 treatment led to a further decrease (42%). This same effect was not observed for the other reductant molecules with CO treatment reaching 55.5% capacity and propene reaching 62.5% of the original capacity.

DRIFT spectra of Ba/Al_2O_3 following various pretreatments and then exposure to NO_2 at 673 K are shown in Fig. 9. The band at 1470 cm^{-1}, also present for the calcined sample (Fig. 9a), is due to $BaCO_3$. Bands at 1620, 1588, and 1557 cm^{-1} following exposure to NO_2 (Fig. 9b) are assigned to nitrate ions on the alumina [10,13–15]. The less readily detected 1470 cm^{-1} band would infer that the formation of nitrates led to at least partial decomposition of $BaCO_3$, or that the intensity of the broad band at 1310 cm^{-1}, due to nitrate species on alumina [14], obscured the band at 1470 cm^{-1}. The latter feature was clearly observed, however, for a sample which had been exposed to SO_2 in N_2 prior to the NO_2 adsorption (Fig. 9c). There was no obvious change in the intensity of bands assigned to adsorbed NO_x compared to the SO_2-free sample, consistent with the NO_x capacity figures (Fig. 8, Table 1) which showed that SO_2 exposure in N_2 did not influence the storage capacity of the support. Following SO_2 in air (Fig. 9d), the band at 1588 cm^{-1} was significantly attenuated but a shoulder at 1370 cm^{-1}, previously undetected, was apparent. Only the samples which had either no previous contact with SO_2 (Fig. 9b) or were treated in SO_2/N_2 (Fig. 9c) showed a resolved feature at ca. 1310 cm^{-1}. All others showed a continuously rising feature below ca. 1400 cm^{-1} with an indication of the shoulder at 1370 cm^{-1} (Fig. 9d–9g). The latter has been assigned to $Al_2(SO_4)_3$ [21,22]. In contrast to the fresh sample, a band at 1155 cm^{-1} (not shown) was obvious for the SO_2-exposed samples. Although often used as a characteristic for bulk $BaSO_4$ [23], the absence of diffraction features [18] for this phase for the Ba/Al_2O_3 (Fig. 1b) suggests that this existed as an amorphous phase or at a low concentration. No reductant was capable of recovering the alumina sites responsible for the band at 1588 cm^{-1} (Fig. 9d–9g).

To distinguish effects which arise due to the presence of Pt from the influence of baria dispersion which can be modified by the addition of Pt precursor [14–16], a portion of Ba/Al_2O_3 was treated with HCl solution, washed with ammonia, and calcined.

TPRS profiles for HCl-treated support (not shown) were qualitatively similar to those of $Pt/Ba/Al_2O_3$. Fig. 10 shows the released NO_x for these samples as a percentage of the storage capacity for the fresh HCl-treated sample. NO_x storage was 0.206 $mmol/g_{cat}$ (Table 1), very similar to the value for the untreated support. Unlike the untreated support (Fig. 8) which was unaffected by a similar treatment, exposure of the HCl-treated Ba/Al_2O_3 to SO_2 in N_2 reduced the NO_x capacity to ca. 70% (Fig. 10). This was qualitatively similar to the result obtained for $Pt/Ba/Al_2O_3$ (Fig. 4). A clear, enhanced influence on the NO_x storage capacity was observed after exposure to SO_2 in air (Fig. 10), where the NO_x capacity was diminished to only 35% of the original value. As observed for the standard Ba/Al_2O_3 support, HCl-treated support, exposure to SO_2 in air and treatment in H_2 reduced the storage capacity even further (30% of the original). CO, on the other hand, did lead to some level of regeneration (41% of the original).

Absence of peaks at 1750 and 1470 cm^{-1} in DRIFT spectra of the HCl-treated support (Fig. 11a) confirm that extensive crystalline $BaCO_3$ was not present possibly due to the well-dispersed barium oxide phase produced after the HCl treatment or that carbonate formation was suppressed due to poisoning of the relevant sites by chloride ions. As for the standard support, bands at 1620, 1588, 1560, and 1310 cm^{-1} appeared after exposure to NO_2 (Fig. 11b). One difference was a band at 1430 cm^{-1}, due to monodentate nitrate on bar-

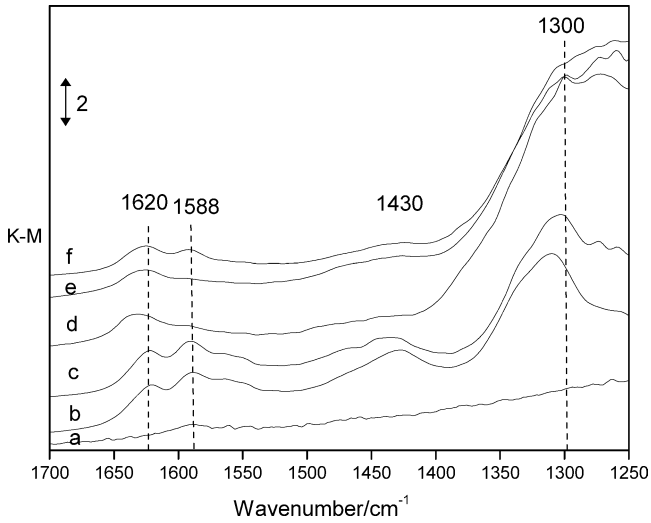

Fig. 11. FTIR spectra of (a) HCl-treated Ba/Al_2O_3 support then after NO_2 exposure between 673 and 298 K for different pretreated samples, (b) without SO_2 treatment, (c) after SO_2 treatment in N_2 at 673 K, and (d)–(f) exposed to SO_2 in air at 673 K with (d) no regeneration or (e) regenerated with H_2 or (f) regenerated with CO.

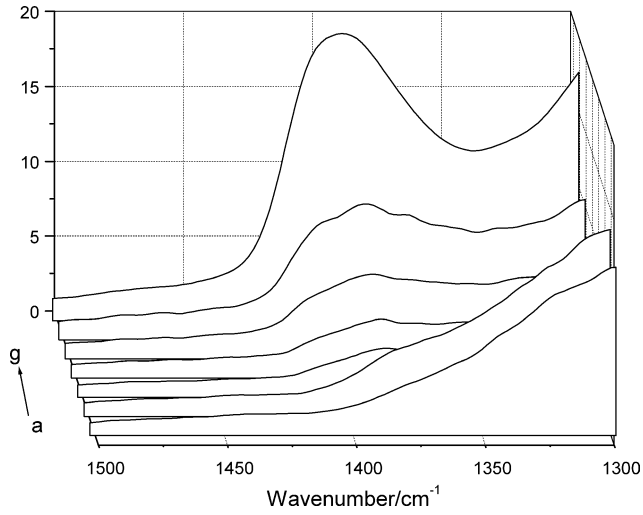

Fig. 12. FTIR spectra of HCl-treated Ba/Al_2O_3 support after SO_2 treatment in air and exposure to 750 ppm NO_2 in N_2/air at 673 K and cooling to 298 K. Sample was heated in 7.98% air/N_2 mixture to 873 K with spectra recorded at (a) 298, (b) 373, (c) 473, (d) 573, (e) 673, (f) 773, and (g) 873 K.

ium [14,19] which was obscured (Fig. 9a) in the spectrum of the standard support by the band at 1470 cm^{-1} due to the carbonate phase. The band at 1430 cm^{-1} was less dominant while the band at 1300 cm^{-1} was slightly increased following exposure of the sample to SO_2 in N_2 (Fig. 11c). As bands at 1620 and 1588 cm^{-1} due to nitrate on the alumina were largely unaffected by this treatment, the loss in NO_x storage capacity resulting from exposure to SO_2 in N_2 (Fig. 10, column 2) must result from loss of centres on the baria component. The loss of intensity at 1588, 1560, and 1430 cm^{-1} due to prior exposure to SO_2 in air (Fig. 11d) indicates that specific sites on the alumina in addition to sites on baria were poisoned by this treatment which resulted in a greater relative loss in NO_x capacity (Fig. 10). An additional modification to the spectrum involved loss of resolution of the 1300 cm^{-1} band which was replaced by a rising background below 1400 cm^{-1} (Fig. 11d). The 1580/1430 cm^{-1} features were not recovered if SO_2 in air was followed by H_2 exposure prior to NO_2 adsorption (Fig. 11e); however, the nitrate species on the alumina giving the band at 1588 cm^{-1} could be reestablished to some extent if CO rather than H_2 was used (Fig. 11f).

Fig. 12 shows IR spectra of HCl-treated support exposed to SO_2 in air at 673 K before exposure to NO_2. As above (Fig. 11d), SO_2 treatment in air followed by exposure to NO_2 led to a spectrum where only the band at 1620 cm^{-1} was apparent, besides the large feature rising from ca. 1400–1250 cm^{-1} (Fig. 11d). If the sample showing these features was then heated to 873 K, the 1620 cm^{-1} band was decreased gradually in intensity and was absent in spectra recorded at 773 K. During heating in air, the feature which had appeared as a rising background below 1400 cm^{-1} was replaced at around 473 K by a band at 1386 cm^{-1} (Fig. 12c) which gained in intensity as a function of temperature (Fig. 12c–12g), reaching a maximum at 873 K. In the absence of other adsorptive species this suggests transformation of a previously adsorbed form of SO_2.

4. Discussion

Under the conditions employed in this study, the degree of poisoning following SO_2 exposure and the extent of recovery of NO_x storage capacity depend on:

(i) Whether SO_2 is introduced in air or nitrogen;
(ii) The presence or absence of Pt;
(iii) The dispersion/chloride washing of baria;
(iv) The choice of reductant.

It will become clear in the following discussion that there is considerable interplay between these factors.

4.1. Adsorption and nature of stored SO_x

Consistent with a previous study [24], gaseous O_2 was not essential for SO_2 storage for the Pt-containing catalyst, with similar suppression of NO_x capacity whether SO_2 was admitted in air or in N_2 (Fig. 4). SO_2 uptake is less for catalysts in the absence of Pt [24], although as the overall NO_x storage capacity was also less in the absence of Pt (Table 1), the influence of this smaller amount of adsorbed SO_2 may have a significant effect on the relative amount of residual NO_x capacity. The presence of O_2 was more significant for Ba/Al_2O_3 in the absence of Pt, with NO_x capacity being reduced to ca. one-half of the level obtained for SO_2 in air compared with SO_2 in N_2 (Figs. 8 and 10). Baria dispersion/Cl retention also played a role as SO_2 in nitrogen had no effect on the, as-prepared, Ba/Al_2O_3 sample whereas

reduced capacity was found for the HCl-washed support (Fig. 10).

Although not essential [24] for storage over $Pt/Ba/Al_2O_3$ (Fig. 4), SO_2 uptake is increased by oxygen due to enhanced SO_3 formation [25] which facilitates bulk sulfate formation [24–27]. XRD indicates bulk $BaSO_4$ formation following exposure of the $Pt/Ba/Al_2O_3$ catalyst to SO_2 in air (Fig. 1d) but this was not detected for Pt-free sample (Fig. 1b). This is consistent with the diminished SO_2 uptake for Pt-free support [20] and would suggest that in the absence of appropriate conditions necessary to convert SO_2 to SO_3 such as the absence of gaseous oxygen or oxidation catalyst, sulfate formation is limited to the surface layers. NO_x capacity may be equally affected irrespective of whether bulk or surface sulfates are formed since NO_x storage is restricted to the surface baria layers [10,11]. Thus SO_2 in N_2 or in air have similar effects on NO_x storage capacity (Fig. 4) for the Pt-containing catalyst even though bulk sulfate is only formed for the latter treatment (Fig. 1d).

4.2. *Influence of adsorbed SO_x on NO_x storage capacity*

Similar degrees of efficiency of SO_2 in N_2 or in air in decreasing NO_x storage capacity could be interpreted as elimination of NO_x storage sites on baria and retention of sites on the alumina since under similar conditions, the latter exhibits ca. 50% of the NO_x storage capacity of a $Pt/Ba/Al_2O_3$ catalyst [14]. However this is at odds with the FTIR results for this sample (Fig. 5) which show that the dominant bands due to stored NO_x appear at 1432 and 1320 cm^{-1} due to nitrates on baria [14,17,20]. Nitrates on alumina appearing as a triplet of bands between 1620 and 1560 cm^{-1} [14,17,20] were not readily detected for $Pt/Ba/Al_2O_3$ (Fig. 5). However, this was also the case whether the catalyst had been exposed to SO_2 (Fig. 5b and 5c) or not (Fig. 5a), indicating that storage by baria rather than by alumina was the dominant process and that SO_2 exposure reduced the capacity to store NO_x (Fig. 4) by interacting with the former either to poison the surface layer (SO_2 in N_2) or to poison surface sites and produce a bulk sulfate species (SO_2 in air).

The greater relative intensity of bands due to nitrate on alumina (1620, 1588, 1310 cm^{-1}) compared with nitrates on baria (1430 cm^{-1}) for both Ba/Al_2O_3 samples (Figs. 9b and 11b) indicates that the alumina made a proportionally greater contribution to the storage capacity of Ba/Al_2O_3 than for $Pt/Ba/Al_2O_3$. SO_2 in air led to diminished NO_x capacities for both untreated (Fig. 8) and HCl-washed Ba/Al_2O_3 (Fig. 10) and this treatment led to partial loss of nitrates on the alumina (1588 and 1560 cm^{-1}) and the overall increased intensity below 1400 cm^{-1}. As chelating bidentate nitrate species on alumina (1588 cm^{-1}) are more thermally stable than other forms of nitrate [14,20], including bridging bidentate nitrate (1620 cm^{-1}) which is the least thermally stable [14] and yet still detected after pretreatment with SO_2 (Figs. 9d and 11d), it is clear that these specific adsorption sites on the alumina are poisoned by the SO_2. Burch et al. [28] noted that SO_2-pretreated Al_2O_3 adsorbed less NO or NO_2, indicating site competition between these species and that a change in desorption temperature occurred for the more strongly adsorbed NO_x. Exposure of the Ba/Al_2O_3 support to SO_2/N_2 led to the appearance of an additional NO_2 desorption feature at ca. 600 K (Fig. 6b) which was not apparent as a resolved feature for the clean support but which was further diminished when SO_2 was admitted in air, with the appearance of an additional component at 440 K (Fig. 6c). It is clear that SO_2 exposure changed qualitative aspects of the stored NO_x as well as the quantitative changes to the storage capacity.

SO_x species responsible for loss of NO_x capacity on alumina have been described [28,29] in terms of surface sulfates giving bands at 1135 and 1070 cm^{-1}. The latter have been ascribed to a surface sulfite on alumina [30]. These studies [30] also indicated that molecularly adsorbed SO_2, detected as a band between 1330 and 1336 cm^{-1}, was observed following low-temperature (300 K) adsorption. As this molecularly adsorbed form of SO_2 is readily removed at 373 K [30], it is unlikely that it would offer such resistance to NO_2 adsorption at 673 K. Stronger bound forms of SO_x on alumina are produced by reacting SO_2 with oxygen at high temperatures with a band at 1350 [4] or ca. 1380 cm^{-1} [22,30] being assigned to the ν(S=O) vibration of $Al_2(SO_4)_3$ [4]. The high thermal stability of this species (Fig. 12g) is consistent with behaviour of aluminum sulfate and sulfated alumina decomposition, the latter showing stability up to and above 873 K [2,24], thus supporting an assignment of the 1386 cm^{-1} band to sulfate on the alumina [22]. Aluminum sulfates are less readily formed than barium sulfate [24], consistent with results here where heating Ba/Al_2O_3 from 298 to 873 K (Fig. 12) following exposure to SO_2 in air at 673 K only led to significant evolution of a band at 1386 cm^{-1} above 673 K reaching maximum intensity at 873 K. Bulk sulfate phases do not show a band at ca. 1380 cm^{-1} [31] and it should be assigned to a surface rather than a bulk sulfate on alumina phase. This is supported by the lack of correlation between this feature and a band at 1035 cm^{-1} with the latter due to the ν(S–O) mode of the bulk phase sulfate [22]. This assignment is consistent with data for other bulk sulfate phases [31] and in distinguishing surface and bulk sulfates formed on ceria [32]. For engine bench-aged monolith catalysts, it is believed [2] that aluminum sulfate exists as a surface layer. The low relative abundance of the surface aluminum sulfate until reaching elevated temperatures (Fig. 12) would suggest that this species was converted from another mode of stored SO_x, which is more likely to have inhibited NO_x storage as nitrate on the alumina (1588/1560 cm^{-1} bands). As barium sulfate has a greater thermal stability than aluminum sulfate [20], this is not thought to be the source of SO_2 for high-temperature formation of sulfate on alumina (Fig. 12). It is more likely that the high-temperature excursion in air converts surface sulfite species (bands below 1200 cm^{-1}) to surface sulfates (1386 cm^{-1}) and that the former are responsible for low-

temperature site blocking and reduced NO_x capacity of the alumina. In the case of ceria [32], sulfates are produced at the expense of sulfite (or hydrogen sulfite) species leading to the loss of bands below 950 cm^{-1}.

Oxidation of SO_2 to SO_3 is facilitated by Pt and sulfate formation is expected at a lower temperature. Loss of NO_x capacity for Pt-containing sample originated in the main from a loss of baria centres, probably reflecting the ease of barium sulfate formation relative to aluminum sulfate [24]. For reducible oxides such as ceria, sulfate formation may occur from SO_2 in the absence of oxygen [32]; however, it is difficult here to explain why NO_x capacity is reduced when SO_2 in N_2 is admitted to $Pt/Ba/Al_2O_3$ (Fig. 4) or HCl-treated Ba/Al_2O_3 (Fig. 10). Again it is possible to invoke a role of a lesser oxidised form of SO_x such as sulfite [32] as dominating during SO_2 exposure, and acting to block NO_x storage sites or being converted to a surface sulfate during subsequent exposure of the samples to NO_2 in air, which then competes for adsorption sites with the NO_2. It should be emphasised that under the conditions employed, formation of bulk aluminum sulfate is negligible (Fig. 1), formation of surface aluminum sulfate is limited (below 673 K; Fig, 12), and so loss/recovery of NO_x storage capacity does not revolve around these species to any significant extent.

4.3. Influence of reductants on the recovery of NO_x storage capacity

Pt plays a significant role in determining the extent to which NO_x capacity is recovered following SO_2/air and then a brief rich cycle. In the absence of Pt, none of the reductants was effective in recovering storage capacity, irrespective of whether standard or HCl-treated support was employed (Figs. 8 and 10). In fact, post hydrogen exposure in the absence of Pt actually enhanced the poisoning effect of SO_2/air whereas in the presence of Pt, complete NO_x storage capacity recovery was achieved (Fig. 4). The efficiency of the regeneration process for Pt-containing catalyst poisoned at 673 K, $H_2 > CO > C_3H_6$ was the same as that observed for catalysts poisoned at 873 K [2]. In the latter example, samples were exposed to the reductant gas in the absence of oxidant, unlike experiments performed here, and H_2S was evolved [2]. XRD shows that H_2 removed the $BaSO_4$ phase (Fig. 1e) while FTIR (Fig. 5d) shows that NO_x storage recovery by the baria component occurred. The mechanism of $BaSO_4$ reduction by H_2 either involves Pt-promoted (hydrogen spillover) reduction to produce BaO, SO_2, and water or BaO, H_2S, and water [2] or sulfate migration from baria to aluminum and hence to the metal site where it undergoes reduction [13]. Additionally, direct sulfate migration from baria to Pt might occur although this would probably be limited to Pt sites at the interface with baria crystallites or in baria-rich regions of the catalyst. Irrespective of the mechanism involved, sulfate reduction by hydrogen may lead to sulphur deposits generated on the Pt under oxygen-deficient conditions [13,27,33]. Note that most regeneration studies of SO_2-treated NSR catalysts involve a rich operating period which involves complete removal of oxygen [2,3,27]. Oxygen in the rich mixture is important as it provides a means of oxidising S deposits on Pt to SO_2 [6,27,33] and under conditions here would appear to prevent formation of a barium sulfide phase [3]. At 673 K oxygen is expected to be fully consumed by H_2 to produce water over these catalysts [20], which is able to hydrolyse S deposits on Pt [9]. As NO storage is less in the absence of Pt (Table 1) [14], full recovery of storage capacity following exposure to SO_2 in air followed by regeneration in H_2/air/N_2 infers that the Pt surface remained S free. Given the greater regeneration efficiency of H_2 compared to CO for $Pt/Ba/Al_2O_3$ (Fig. 4), we concur [13] that water is a key component in the regeneration of the catalyst.

Water formation from H_2 oxidation is less likely in the absence of Pt and regeneration is expected [13] to be less effective. Both Pt-free supports showed worse NO_x capacity following SO_2/air then H_2/air/N_2 than if the latter treatment were omitted (Figs. 8 and 10). Although barium sulfate may be converted to sulfide in H_2 at temperatures above 623 K giving a peak at $2\theta = 24.1°$ in XRD patterns [3], the lack of XRD evidence for a crystalline sulfate phase for the support (Fig. 1b) would make it unlikely that BaS would be detected here. This sulfide phase was stable up to 1073 K in H_2/N_2 [3] but might be expected to convert to a more oxidised state when heating in an oxidising atmosphere. This would be consistent with FTIR data (Fig. 12) where the surface aluminum sulfate phase (1386 cm^{-1}) was detected for the support heated in air above 673 K. An alternative to oxidation of the sulfide phase involved displacement by carbonate in the presence of CO_2 [3]. Ba/Al_2O_3 in the absence of Pt showed activity for CO oxidation at 673 K [34], suggesting that CO_2 may have been a component of the gas phase under these conditions. Note that both support samples showed greater recovery of NO_x capacity following heating in CO compared with H_2 (Figs. 8 and 10). However, FTIR spectra do not show (Figs. 9f and 11f) enhanced carbonate formation (1470 cm^{-1}) following exposure to CO/air compared to hydrogen/air-treated samples (Figs. 9e and 11e) or to the support where no attempt was made to regenerate (Figs. 9d and 11d) and thus displacement of a reduced form of stored S by preferential carbonate formation [3] would not appear to explain the limited (Table 1), but reproducible, improvement in NO_x capacity following treatment in this gas mixture. These same spectra show recovered intensity at 1588 cm^{-1} following exposure to CO/air (Figs. 9f and 11f) which was not achieved in H_2/air (Figs. 9e and 11e) and differences in NO_x capacity following CO/air compared to the H_2/air may originate in the recovery of chelating bidentate nitrate sites [14] on the alumina.

As for higher sulfation temperatures elsewhere [2,3,13], CO was less effective than H_2 in recovering NO_x capacity for the SO_2-treated Pt-containing sample (Table 1, Fig. 4). One could ascribe this difference to the relative ability of the two reductants to interact directly with the sulfate group on

baria, which, for the Pt-containing sample, was the principle location of NO_x storage sites (Fig. 5). However, Limousy et al. [13] have shown that unless water is included in the feed gas, CO does not produce H_2S or COS over a sulfated NO_x trap, while in the presence of water, high emissions of H_2S are detected. The latter assumes that in the absence of water, metal sulfides are formed under rich conditions [13,27,33] which prevent subsequent sulfate reduction and recovery of NO_x capacity. A weak band at 2115 cm^{-1} due to CO adsorbed at oxidised Pt centres was observed following SO_2 in air at 673 K and then CO followed by exposure to NO_2. This may reflect the relative strengths of CO adsorbed at oxidised sites compared to Pt^0 [35] with CO being readily displaced at 673 K by NO_2 in the gas stream rather than indicating blockage of the latter sites by S residues. Amberntsson et al. [27] also failed to observe CO adsorbed on Pt^0 sites after exposing the catalyst to SO_2 at 673 K, suggesting that poisoning of the Pt sites by S may be significant.

Propene in He at 623 K had negligible effects on IR band intensities of sulfate species [4] and this was the least effective of the three reductant gases used here for the $Pt/Ba/Al_2O_3$ sample. SO_2 on Pt is highly reactive with C_3H_6 resulting in S deposits on Pt [36]. In the absence of SO_2 and under excess oxygen conditions, the catalyst used here is highly active for propene oxidation at 673 K [20]. As outlined above, both water [13] and CO_2 [3] are beneficial in regenerating NO_x storage capacity of SO_2-poisoned catalysts and it might be assumed that combustion products were not present in significant concentrations under the rich propene/air/nitrogen pulse. Similarly, propene decomposition to yield H_2 was also apparently insignificant given the efficiency of the latter to regenerate SO_2-treated $Pt/Ba/Al_2O_3$ (Fig. 4). The minor recovery of NO_x capacity for the Pt-free sample following treatment in propene can be attributed, as for CO, to the recovery of sites where NO_x was adsorbed as a chelating nitrate (1588 cm^{-1}) on the alumina (Fig. 9g). A conclusion which could be drawn from the limited success in recovering NO_x storage capacity for the Pt-free samples (Figs. 8 and 10) is that the reductant molecules are inefficient at directly reducing the sulfate or other forms of adsorbed SO_x. This provides some support for a mechanism involving migration of a sulfate unit (or other form of stored SO_x) from baria to the noble metal via the alumina surface [13,25] followed by reduction on the metal site, the retention of an S atom, and eventually deactivation in the absence of water. The alternative that reductant is activated on the metal and transferred to the support might lead to an equivalent scenario if the H_2S released [13] then interacts with the Pt releasing H_2 and retaining S. Experiments to distinguish between the two pathways are in progress [34].

5. Conclusions

Exposure of SO_2 at 673 K leads to loss of NO_x storage capacity due to formation of barium sulfate and other S-containing species on the support. In the presence of Pt, the former makes the greatest contribution to loss of NO_x capacity whereas for the support alone, SO_x adsorption on the alumina makes a significant contribution to lost NO_x uptake. Sulfates on the alumina are only formed in large quantities at higher ($T > 673$ K) temperatures. In the presence of Pt the order of regeneration efficiency was $H_2 > CO >$ propene while in contrast hydrogen was least effective in the absence of Pt. The presence of oxygen during the rich regeneration period appears be significant as this allows formation of water which has the potential to hydrolyse S residues on the noble metal. The use of hydrogen at low temperatures to release and reduce stored NO_x has the potential to limit sulfate buildup and thus limit the extent to which deactivation due to growth of barium sulfate particles take place and to avoid thermal degradation of the catalyst which accompanies high-temperature desulfation.

Acknowledgments

We thank the Royal Society (London) for provision of a K.C. Wong Fellowship (to Z.L.) and Dr. Bill Epling (Cummins, Inc.) for helpful comments on the manuscript.

References

[1] N. Takahashi, H. Shinjoh, T. Iijima, T. Suzuki, K. Yamazaki, K. Yokota, H. Suzuki, N. Miyoshi, S. Matsumoto, T. Tanizawa, S. Tanaka, T. Tateishi, K. Kashara, Catal. Today 27 (1996) 63.
[2] S. Matsumoto, Y. Ikeda, H. Suzuki, M. Ogai, N. Miyoshi, Appl. Catal. 23 (2000) 115.
[3] S. Pouston, R.R. Rajaram, Catal. Today 81 (2003) 603.
[4] Ch. Sedlmair, K. Seshan, A. Jentys, J.A. Lercher, Catal. Today 75 (2002) 413.
[5] J. Parks, A. Watson, G. Campbell, B. Epling, SAE technical paper series 2002-01-2880 (2002).
[6] Y. Takahashi, Y. Takeda, N. Kondo, M. Murata, SAE technical paper series 2004-01-0580 (2004).
[7] Y. Cheng, J.V. Cavataio, W.D. Belanger, J.W. Hoard, R.H. Hammerle, SAE technical paper series 2004-01-0156 (2004).
[8] E. Fridell, M. Skoglundh, SAE technical paper series 2004-01-0080 (2004).
[9] C. Courson, A. Khalfi, H. Mahzoul, S. Hodjati, N. Moral, A. Kiennemann, P. Gilot, Catal. Commun. 3 (2002) 471.
[10] J.A. Anderson, M. Fernández-García, Ind. Chem. Eng. 78A (2000) 935.
[11] D. James, E. Fourré, M. Ishii, M. Bowker, Appl. Catal. B 45 (2003) 147.
[12] K. Yamazaki, T. Suzuki, N. Takahashi, K. Yokota, M. Sugiura, Appl. Catal. B 30 (2001) 459.
[13] L. Limousy, H. Mahzoul, J.F. Brilhac, F. Garin, G. Maire, P. Gilot, Appl. Catal. B 45 (2003) 169.
[14] J.A. Anderson, B. Bachiller Baeza, M. Fernández-García, Phys. Chem. Chem. Phys. 5 (2003) 4418.
[15] J. Dawody, M. Skoglundh, E. Fridell, J. Mol. Catal. 209 (2004) 215.
[16] A. Sepulveda-Escribano, M. Primet, H. Praliaud, Appl. Catal. 108 (1994) 221.
[17] Ch. Sedlmair, K. Seshan, A. Jentys, J.A. Lercher, J. Catal. 214 (2003) 308.
[18] Daresbury Crystallographic Database, File 7024-Barium Sulphate.
[19] J.A. Anderson, A.J. Paterson, M. Fernández-García, Stud. Surf. Sci. Catal. 130 (2000) 1331.

[20] Z. Liu, J.A. Anderson, J. Catal. 224 (2004) 18.
[21] D. Uy, A. Dubkov, G.W. Graham, W.H. Weber, Catal. Lett. 68 (2000) 25.
[22] D. Uy, K.A. Wiegand, A.E. O'Neil, M.A. Dearth, W.H. Weber, J. Phys. Chem. B 106 (2002) 387.
[23] H. Mazhzoul, J.F. Brilhac, P. Gilot, Appl. Catal. B 20 (1999) 47.
[24] H. Mahzoul, L. Limousy, J.F. Brilhac, P. Gilot, J. Anal. Appl. Pyrolysis 56 (2000) 179.
[25] L. Limousy, H. Mahzoul, J.F. Brilhac, P. Gilot, F. Garin, G. Maire, Appl. Catal. B 42 (2003) 237.
[26] E. Fridell, H. Persson, L. Olsson, B. Westerberg, A. Amberntsson, M. Skoglundh, Top. Catal. 16/17 (2001) 133.
[27] A. Amberntsson, M. Skoglundh, S. Ljungstrom, E. Fridell, J. Catal. 217 (2003) 253.
[28] R. Burch, E. Halpin, J.A. Sullivan, Appl. Catal. B 17 (1998) 115.
[29] R. Burch, T.C. Watling, Appl. Catal. B 17 (1998) 131.
[30] M.A. Babaeva, A.A. Tsyganenko, V.N. Filimonov, Kinet. Catal. 25 (1994) 921.
[31] S.D. Ross, in: V.C. Farmer (Ed.), Infrared Spectra of Minerals, Mineralogical Society, London, 1974, p. 423.
[32] M. Waqif, P. Bazin, O. Saur, J.C. Lavalley, G. Blanchard, O. Touret, Appl. Catal. B 11 (1997) 193.
[33] A. Amberntsson, M. Skoglundh, M. Jonsson, E. Fridell, Catal. Today 73 (2002) 279.
[34] Z. Liu, J.A. Anderson, Unpublished results.
[35] J.A. Anderson, Catal. Lett. 13 (1992) 363.
[36] K. Wilson, C. Hardacre, C.J. Baddeley, J. Lüdecke, D.P. Woodruff, R.M. Lambert, Surf. Sci. 372 (1997) 279.